Supplemental Table of Contents

Table S13 – Putative distal enhancer regions parsed as being TTX-specific based on H3K27ac signal

Table S14 – Loops called on mouse ES cell HiC from Bonev et al. 2017

Table S15 – Loops called on mouse NPC HiC from Bonev et al. 2017

Table S16 – Loops called on mouse cortical neuron (CN) HiC from Bonev et al. 2017

Table S17 - Loops called on human cortical plate (CP) tissue HiC from Won et al. 2016

Table S18 - Loops called on human germinal zone (GZ) tissue HiC from Won et al. 2016

Table S19 - Classified genes opposite disease-Associated SNVs

Supplemental Methods

Cell Culture

Murine cortical neurons were cultured using a protocol established previously in [1]. Briefly, cortices were dissected from E18 WT C57/BL6 mouse embryos. Cortices were then dissociated in DNase (0.01%; Sigma-Aldrich, St. Louis, MO) and papain (0.067%; Worthington Biochemicals, Lakewood, NJ), then triturated with a fire-polished glass pipette to obtain a single-cell suspension. Cells were pelleted at 1000xg for 4 min, the supernatant removed, and cells resuspended and counted with a TC-20 cell counter (Bio-Rad, Hercules, CA). Neurons were plated in 6-cm dishes (Greiner Bio-One, Monroe, NC) coated with poly-L-lysine (0.2 mg/mL; Sigma-Aldrich) at a density of 200,000 cells/mL. Neurons were initially plated in Neurobasal media containing 5% horse serum (NM5), 2% GlutaMAX, 2% B-27, and 1% penicillin/streptomycin (Thermo Fisher Scientific) in a 37ºC incubator with 5% CO2. On DIV4, neurons were fed via half media exchange with astrocyte-conditioned Neurobasal media containing 1% horse serum (NM1), GlutaMAX, and penicillin/streptomycin, 2% B-27, and 5 μM cytosine β-D-arabinofuranoside (AraC; Sigma-Aldrich). Neurons were fed with astrocyte-conditioned NM1 media every three days thereafter. For chronic activity experiments, neurons were treated for 24 hours with either 1 uM Tetrodotoxin (TTX) or 10 uM Bicuculline (Bic) at DIV15 via addition to the cell culture media or left untreated. For short-term activity induction experiments, samples were subjected to 24 hours of TTX treatment at DIV15 followed by 0, 5, 20, 60, or 360 min of Bic treatment on DIV16. All animal experiments were approved by the Institutional Animal Care and Use Committee of the University of Utah.

ChIP-seq library preparation

At DIV16, neuronal cultures were fixed in 1% formaldehyde for 10 minutes (room temp) via the addition (1:10 vol/vol) of the following fixation solution: 50 mM Hepes-KOH (pH 7.5), 100 mM NaCl, 1 mM EDTA, 0.5 mM EGTA, 11% Formaldehyde. Fixation was quenched via the addition of 2.5 M glycine (1:20 vol/vol) and scraped into pellets of 8 million cells. Each pellet was washed once with cold PBS, flash frozen, and stored at -80ºC. Immunoprecipitation was performed as described previously[2, 3] with slight modifications. Briefly, IP reactions were prepared a day prior to cell lysis by combining 20 uL of protein A and protein G conjugated agarose beads (Invitrogen# 15918-014 and 15920-010, respectively) with 10 uL of anti-H3K27ac antibody (Abcam# ab4729, lot GR3187598-1, validated for ChIP by company) in 1 mL of cold PBS and rotated overnight. The next day cell pellets were resuspended in 1 mL lysis buffer (10 mM Tris pH 8.0, 10 mM NaCl, 0.2% NP-40/Igepal, Protease Inhibitor, PMSF) and incubated on ice for 10 min. Cells were further lysed with 30 strokes of a dounce homogenizer (pestle A) and then nuclei were pelleted. Nuclei were lysed on ice in 50 mM Tris pH 8.0, 10 mM EDTA, 1% SDS, Protease Inhibitor, PMSF for 20 min. SDS concentration was reduced before sonication by the addition of 300 uL IP Dilution Buffer (20 mM Tris pH 8.0, 2 mM EDTA, 150 mM NaCl, 1% Triston X-100, 0.01% SDS, Protease Inhibitor, PMSF), after which samples were sonicated for 60 minutes (30 seconds on, 30 seconds off cycle, 100% amplitude) using a Qsonica Q800R2 Sonicator. Insoluble fractions were removed via spin, and the supernatant was removed of non-specific binding chromatin via rotation with preclearing solution (3.7 mL IP Dilution Buffer, 0.5 mL Nuclear Lysis Buffer, 175 uL of Agarose Protein A/G beads, and 50 ug Rabbit IgG) for 2 hours at 4°C. Beads were pelleted and 4.7 mL of supernatant was removed. 200 uL of supernatant was retained as input control (stored at -20°C) while the remaining 4.5 mL was transferred to the beads that had been pre-bound with the H3K27ac antibody overnight; the IP reaction then rotated overnight again at 4°C. Bound bead complexes were washed once with 1 mL IP Wash Buffer 1 (20 mM Tris pH 8.0, 2 mM

EDTA, 50 mM NaCl, 1% Triton X-100, 0.1% SDS), twice with 1 mL High-Salt Buffer (20 mM Tris pH 8.0, 2 mM EDTA, 500 mM NaCl, 1% Triton X-100, 0.01% SDS), once with IP Wash Buffer 2 (10 mM Tris pH 8.0, 1 mM EDTA, 0.25 M LiCl, 1% NP-40/Igepal, 1% Na-deoxycholate), and finally twice with 1x TE. Complexes were eluted by twice resuspending bound beads in 110 uL Elution Buffer (100 mM NaHCO3, 1% SDS), pelleting the beads after each elution and transferring 100 uL supernatant to a new tube. Finally, 12 uL of 5M NaCl and 20 ug RNase A were added to both 200 uL IP and input samples and incubated at 65 degrees for 1 hour, followed by the addition of 60 ug of Proteinase K and overnight incubation at 65 degrees. DNA was isolated via phenol-chloroform extraction and ethanol precipitation and concentration was quantified using Qubit fluorometer.

ChIP-seq libraries were prepared for sequencing using the NEBNext Ultra II DNA Library Prep Kit (NEB# E7645S), following manufacturer's protocol with the following user-chosen specifications. 3 ng DNA from all IP and input samples was used as starting material. NEBNext Adaptors were diluted 15x in 10 mM Tris-HCL, pH 8.0 with 10 mM NaCl prior to adaptor ligation. Large DNA fragments were removed via a size selection by adding 15 uL of AMPure XP beads at the first bead addition step and 87 uL of beads at the second bead addition step. Size-selected DNA was amplified using 9 cycles of PCR enrichment. The size-range of the final libraries was confirmed to be between 200-1000 bp using an Agilent Bioanalyzer High Sensitivity DNA test. H3K27ac enrichment was confirmed prior to sequencing by querying the IP/input qPCR enrichment of primer pairs designed to the Arc, Synaptotagmin-1, and Tcf25 promoter regions. Library concentrations were calculated and normalized using the KAPA Illumina Library Quantification Kit (#KK4835) so that libraries could be equally pooled before sequencing 75 bp single-end reads on the NextSeq500. IP libraries were sequenced to a depth greater than 48 million reads and all input libraries were sequenced to greater than 67 million reads.

ChIP-seq Analysis

H3K27ac ChIP-seq reads were aligned to the mm9 genome using Bowtie[4]. Reads with more than two possible alignments were removed (-m2 flag utilized). IP libraries across the Bic, Untreat, and TTX conditions were downsampled to 38 million reads, while input libraries were downsampled to 44 million reads. Peaks were identified using MACS2[5] with a p-value cutoff parameter of $1x10e^{-8}$ and the broadpeak flag also invoked with a broadpeak cutoff of $1x10e^{-8}$.

Parsing Putative Activity-Dependent Enhancers

H3K27ac peaks (p-value, broadPeak thresholds = $1x10^{-8}$) called in the TTX and Bic conditions were concatenated together and peaks within 2 kb of RefSeq TSS's were removed. The remaining peaks were merged so that peaks within 10 kb of each other were also merged together, thus generating a list of enhancer sites shared across the Bic and TTX conditions. From this master list of enhancer sites, each was parsed into activity-response classes by (i) calculating the average bigwig signal across the enhancer interval using the pybigwig package in both the Bic and TTX IP libraries, (ii) dividing those signal averages by the average signal in the corresponding input library, (iii) calculating the Bic/TTX fold change of those input-normalized enhancer signals. An enhancer was defined as Bic-specific (activity-induced) if it exhibited a >2 Bic/TTX fold change and its Bic input-normalized signal was in the top 80% of all enhancers; TTX-specific (activity-decommissioned) enhancers were defined in the same manner with the conditions reversed. The remaining enhancer sites were classified as constitutive (activity-invariant) if their Bic and TTX input-normalized signals fell in the top 80% of enhancer signals in both conditions. H3K27ac signal heatmaps for each enhancer class were plotted using the Deeptools package[6].

3C Template Generation

Neuronal cultures were formaldehyde fixed as described for ChIP-seq and stored at -80ºC. For each condition (Bic, Untreat, TTX), *in situ* 3C was performed on 4 replicates (divided evenly across two animal/culture batches) of 4-5 million cells as described previously[2, 7-9]. Briefly, cells were thawed on ice and resuspended (gently) in 250 uL of lysis buffer (10 mM Tris-HCl pH 8.0, 10 mM NaCl, 0.2% Igepal CA630) with 50 uL protease inhibitors (Sigma P8340). Cell suspension was incubated on ice for 15 minutes and pelleted. Pelleted nuclei were washed once in lysis buffer (resuspension and spin), then resuspended and incubated in 50 uL of 0.5% SDS at 62ºC for 10 min. SDS was inactivated via the addition of 145 uL H_2O, 25 uL 10% Triton X-100, and incubation at 37ºC for 15 min. Subsequently, chromatin was digested overnight at 37ºC with the addition of 25 uL 10X NEBuffer2 and 100U (5 uL) of HindIII (NEB, R0104S), followed by 20 min incubation at 62ºC to inactivate the HindIII. Chromatin was re-ligated via the addition of 100 uL 10% Triton X-100, 120 uL NEB T4 DNA Ligation buffer (NEB B0202S), 12 uL 10 mg/mL BSA, 718 uL H_2O, and 2000 U (5 uL) of T4 DNA Ligase (NEB M0202S) and incubation at 16ºC for 2 hours (NOTE: This is a deviation from in situ HiC (Rao et al. 2010) in order to promote sticky-end ligation over blunt-end). Following ligation nuclei were pelleted, resuspended in 300 uL of 10 mM Tris-HCl (pH 8.0), 0.5 M NaCl, 1% SDS, plus 25 uL of 20 mg/mL proteinase K (NEB P8107), and incubated at 65ºC for 4 hours at which point an additional 25 uL of proteinase K was added and incubated overnight. 3C templates were isolated next day via RNaseA treatment, phenol-chloroform extraction, ethanol precipitation, and Amicon filtration (Millipore MFC5030BKS) (for more details see[2, 3]). Template size distribution and quantity were assessed with a 0.8% agarose gel.

5C Library Preparation

5C primers were designed according to the double-alternating design scheme[7, 10-12] using the My5C primer design software (http://my5c.umassmed.edu/my5Cprimers/5C.php)[13] with universal "Emulsion" primer tails. Regions were designed to capture TAD structures immediately surrounding the genes of interest (Bdnf, Fos, Arc, Neurexin-1, Neuroligin-3, Synaptotagmin-1) in published mouse cortex HiC data[14]. 5C reactions were carried out as previously described[7, 11, 12]. 600 ng (~200,000 genome copies) of 3C template for each replicate was mixed with 1 fmole of each 5C primer and 0.9 ug of salmon sperm DNA in 1x NEB4 buffer, denatured at 95ºC for 5 min, then incubated at 55ºc for 16 hours. Primers which had then annealed in adjacent positions were ligated through the addition of 10 U (20 uL) Taq ligase (NEB M0208L) and incubation at 55ºC for 1 hour then 75ºC for 10 min. Successfully ligated primer-primer pairs were amplified using primers designed to the universal tails (FOR = CCTCTC TATGGGCAGTCGGTGAT, REV = CTGCCCCGGGTTCCTCATTCTCT) across 30 PCR cycles using Phusion High-Fidelity Polymerase. Presence of a single PCR product at 100 bp was confirmed via agarose gel, then residual DNA <100 bp was removed through AmpureXP bead cleanup at a ratio of 2:1 beads:DNA (vol/vol). 100 ng of the resulting 5C product was prepared for sequencing on the Illumina NextSeq 500 using the NEBNext Ultra DNA Library Prep Kit (NEB E7370) following the manufacturer's instructions with the following parameter selections: during size selection, 70 uL of AMPure beads was added at the first step and 25 at the second step; linkered fragments were amplified using 8 PCR cycles. A single band at 220 bp in each final library was confirmed using an Agilent DNA 1000 Bioanalyzer chip, and library concentration was determined using the KAPA Illumina Library Quantification Kit (#KK4835). Finally, libraries were evenly pooled and sequenced on the Illumina NextSeq 500 using 37 bp paired-end reads to read depths of between 11 and 30 million reads per replicate.

5C Interaction Analysis

The adoption of the double alternating primer scheme and *in situ* 3C significantly improved 5C data quality (see Kim and Titus 2018[7] for more detail) such that some steps of our 5C analysis approach could be changed from those previously utilized[2, 3] to more closely resemble those used for analyzing HiC[8]. Paired-end reads were aligned to the 5C primer pseudo-genome using Bowtie, allowing only reads with one unique alignment to pass filtering. Only reads for which one paired end mapped to a forward/left-forward primer and the other end mapped to a reverse/left-reverse primer were tallied as true counts.

5C is subject to specific biases, such as primer GC content resulting in annealing/PCR biases, that methods such as HiC are not. This manifests in primer-primer pairs with mapped counts that are orders of magnitude higher than the neighboring primer-primer pairs. Such an extreme enrichment of single primer-primer pairs does not resemble the broader distribution of elevated counts, spanning clusters of neighboring primer-primer pairs, that exists at bona fide looping interactions across 5C and HiC data. Therefore, we decided to remove these biased primer-primer pairs before proceeding with interaction analysis. This was done by calculating for each primer-primer pair the median count of itself and the 24 primer-primer pairs nearest to the primer-primer pair in question (i.e. a scipy.ndimage.generic_filter window of size 5 was passed over the primer-primer pair matrix and the median of each window was recorded). If the count of one primer-primer pair was greater than eight-fold higher its neighborhood median then it was flagged as a high spatial outlier and removed. This process was performed for all primer-primer pairs, except for those in the 5C region surrounding the Arc gene for which the 8-fold threshold was found to be too stringent due to low region complexity and a 100-fold threshold was utilized instead.

After high-outlier removal, primer-primer pair counts were quantile normalized across all 12 replicates (4 per condition) as previously described[7, 15]. For plotting purposes quantile normalized counts were merged across replicates via summation, whereas for loop calling analysis all replicates were kept separate. Primer-primer pair counts were then converted to fragment-fragment interaction counts by averaging the primer-primer counts that mapped to each fragment-fragment pair (max of 2 if both a forward/left-forward and a reverse/left-reverse primer were able to be designed to both fragments and were not trimmed during outlier removal). We then divided our 5C regions into adjacent 4 kb bins and computed the relative interaction frequency of two bins (i,j) by summing the counts of all fragment-fragment interactions for which the coordinates of one of the constituent fragments overlapped (at least partially) a 12 kb window surrounding the center of the 4 kb i^{th} bin and the other constituent fragment overlapped the 12 kb window surrounding the center if the j^{th} bin. Binned count matrices were then matrix balanced using the ICE algorithm[15, 16], at which point we considered each entry (i,j) to represent the 'Relative Interaction Frequency' of the 4 kb bins i and j. Finally, the background contact domain 'expected' signal was calculated using the donut background model as previously described[14] and used to normalize the relative interaction frequency data for the background interaction frequency present at each bin-bin pair. The resulting background-normalized interaction frequency ("observed over expected") counts were fit with a logistic distribution from which p-values were computed for each bin-bin pair and converted into 'Background-corrected Interaction Scores' (interaction score = $-10*\log_2$(p-value)) as previously described[2]. Interaction scores have proven to be informatively comparable across replicates and conditions[2, 17], and as such were used for most visualization analysis and all loop-calling analysis to follow.

Quantitative 5C Loop Identification

We applied the 3DeFDR analysis package[18] to our dataset in order to identify differential interactions across the TTX and Bic conditions (4 replicates of each). Briefly, 3DeFDR identifies differential interactions and empirically estimates a false discovery rate (eFDR) for each identified dynamic looping class. Interactions are only considered for analysis if the interaction scores of all 8 replicates across both conditions surpassed a 'significance threshold'. Interactions are classified as 'TTX-only' if all 4 interaction scores of the TTX replicates surpassed the interaction scores of the Bic replicates by more than a specified 'difference threshold'. 'Bic-only' interactions are classified in the same manner. Those interactions that pass the significance threshold but are not classified as Bic-only or TTX-only are classified as 'Constitutive'. Finally, significant interactions that pass our thresholds are clustered based on spatial adjacency into 'loops'. Looping clusters smaller than 5 pixels were removed. The 3DeFDR package simulates null replicate sets (i.e. 8 replicates of the same cell type/condition) using on a negative binomial counts generating function parameterized with mean-variance relationships computed from the real data. We compute an empirical FDR (eFDR) for each differential loop class as the total number of significant interactions called in that class on a simulated null replicate set divided by the total number of significant interactions called as that class with the original real replicate set.

We utilized the 'non-adaptive' functionality option of the 3DeFDR analysis package, which sweeps across a wide range of difference threshold and calculates an eFDR for each loop class at each iteration. We generated 250 simulated null replicate sets of 8 replicates based on mean-variance relationships underlying the real TTX replicates. We utilized the default 3DeFDR initialization parameters with the exception of 'bin_properties', which is a tunable parameter that specifies the distance scales over which fragment level interactions are stratified prior to fitting the negative binomial counts generating function to those interactions. We modified 'bin_properties' to capture the full extent of our regional matrices: (1) for close-range interactions (0-150 kb), we stratified the interactions using fine-grained, 12 kb-sized sliding windows with a 4 kb step, (2) for mid-range interactions (151-600 kb), we stratified the interactions into 24 kb-sized sliding windows with an 8 kb step, and (3) for longer range interactions (601-2500 kb), we stratified the interactions into coarse-grained, 60 kb-sized sliding windows with a 24 kb step. Through this approach we achieved an eFDR of 6.6% for Bic-only (activity-induced) loops utilizing a difference threshold of 6.75, a significance threshold of $-10*\log_2(0.08)$ (i.e. a p-value of 0.08 resulting from the logistic fit to the observed over expected data), and a cluster size threshold of 5.

RNA-seq library preparation

At DIV5 and DIV16, 900,000 neurons were lysed in 1 mL Trizol (Thermo Fisher Scientific 15596026). Lysates were snap frozen and stored at -80^{o}c until use. Total RNA was then isolated using the mirVana miRNA Isolation Kit (Thermo Fisher Scientific AM1561) according to manufacturer's protocol and eluted from the spin-column using 100 uL nuclease-free water. Samples were DNase treated (Thermo Fisher Scientific AM1906) and tested for quality using an Agilent Bioanalyzer RNA chip. All samples produced an RNA Integrity Number (RIN) greater than 9. To avoid poly-A selection, we utilized the TruSeq Stranded Total RNA Library Prep Kit with Ribo-Zero Gold (Illumina RS-122-2301) and prepared each RNA sample for sequencing according to the manufacturer's protocol. cDNA libraries were amplified across 15 PCR cycles followed by AMPure XP Bead clean-up (1:1 bead:solution ratio). Finally, the library sizes were confirmed to be between 200-500 bp using the BioAnalyzer before sequencing 75 bp paired-end reads on the Illumina NextSeq500. To minimize and identify technical variation, three replicates spanning two culture batches were prepared, pooled, and sequenced to depths of greater than 60 million reads per library.

RNA-seq analysis

RNA-seq reads were mapped to the RefSeq transcriptome (transcriptome fasta downloaded from the UCSC genome browser on July 28, 2017) using Salmon[19]. In accordance with the TruSeq Stranded Total RNA Library Preparation, mapping was done using the -ISR flag. Additionally, 100 bootstraps of transcript quantification were performed. The resulting TPM quantifications for each RefSeq transcript were utilized for all downstream analyses (**Figures 1-4, Table S3**). The Wasabi package (https://github.com/COMBINE-lab/wasabi) was utilized to convert Salmon bootstraps to the format necessary for differential expression analysis by Sleuth[20]. Differentially expressed transcripts were called using the Sleuth wald test, with a q-value threshold of 0.05 (**Table S4**). For enhancer RNA (eRNA) analysis, RNA-seq reads were mapped to the mm9 genome using STAR version 2.7.1[21] using default settings. Resulting bigwig files were used to quantify RNA signal overlapping each enhancer interval.

Linear Regression Modeling

To assess the relative contributions of cis-regulatory elements to activity response gene expression, for each transcript in our 5C regions we sought to quantify its promoter activity, looping strength, looped enhancer activity, and nearby enhancer activity. Transcripts whose promoter fell within 200kb of the edge of a 5C region were removed due to incomplete/truncated ability to query loops outside the 5C regions. Additionally, if transcripts of the same gene had overlapping promoters (+/- 2kb from TSS), only the transcript with the highest maximum expression (TPM) across the TTX and Bic RNA-seq replicates was carried forward for further analysis. The promoter activity of each gene was calculated using the PyBigWig package to find the $\log_2$(Bic/TTX) fold change of the sum H3K27ac bigwig signal across the 4 kb promoter (+/- 2kb from TSS) in each condition (**Figure 2a,f**).

Each transcript was paired with the enhancer nearest to its TSS along the linear genome. If no enhancers fell within 200kb of the promoter, the transcript was considered to have no 'near enhancer' (only the case for NM_026271). The "activity" of the near enhancers were then also calculated as the $\log_2$(Bic/TTX) fold change of the sum H3K27ac bigwig signals across the enhancer (**Figure 2g**). Additionally, the total interaction frequency for each promoter was calculated by summing the observed 5C counts in the Bic and TTX conditions of all 5C bins the promoter overlapped and calculating the $\log_2$(Bic/TTX) fold change (**Figure 2b**). Similarly, the promoter of each transcript was intersected with 5C loops so that it could be paired with enhancers that fell at the other anchor of each loop. Often, promoters formed several loops, interacting with multiple enhancers. To select the single enhancer-promoter loop (so that we could accurately compare to the single nearest enhancer) predicted to have the largest regulatory role on the gene in question, we leveraged an adapted 'ABC model' approach originally reported by Engreitz and colleagues[22], selecting the enhancer-promoter loop that had the highest ((H3K27ac signal) * (5C Obs/Exp)) value (**Figure 2c**). Only promoters that looped to enhancers were included in calculations of loop strength and looped enhancer signal (**Figure 2d-e, 2h-i**). Notably, the looped enhancer models were more predictive of activity-dependent gene expression than the nearest enhancer and promoter-only models, and this trend remained whether we used only genes engaged in loops (N=45, **Supp. Figure 6b-e**) or all genes (N=69, **Figure 2d-e, 2h-i**). 'Loop strength' was then calculated as the $\log_2$(Bic/TTX) fold change of the 5C Obs/Exp counts of the ABC prioritized loop for each gene (**Figure 2d,h**). 'Looped enhancer' signal was calculated as the $\log_2$(Bic/TTX) fold change of the sum H3K27ac bigwig signal in each condition at the selected looped enhancer (**Figure 2e,i**). Finally, the ((H3K27ac signal) * (5C Obs/Exp)) score itself was used to build a regression model (**Figure 2j**). The expression fold change of each transcript was calculated as the $\log_2$(Bic/TTX) fold change of the transcripts per million (TPM) estimate provided by the Salmon

quantification algorithm (a pseudocount of 1 was added to the TPM expression counts in each condition before log transformation). Representative boxplots depict: center line, median; box limits, upper and lower quartiles; whiskers, 1.5x interquartile range; points, outliers.

For linear regression modeling, the vectors of each epigenetic feature described in the prior paragraphs were min-max scaled to a range of -0.5 to 0.5 using the sklearn.preprocessing minmax_scale function so that the calculated coefficients of each model could be compared to each other. The ordinary least squares function of the statsmodels.formula.api package was then used to generate linear regression models from combinations of these epigenetic features as explanatory variables and expression fold change as the response variable. Residuals were plotted to confirm approximate normal distributions. The performances of these models were evaluated by the coefficient (slope) and significance of each term (**Figure 2k**) and the percent of the transcriptional variance explained (R^2) of each model (**Figure 2l**).

HiC Pre-processing

Mouse[23] and human[24] paired-end reads were aligned to the mm9 and hg19 genomes, respectively, using bowtie2[25] (global parameters:–very-sensitive –L 30 –score-min L,-0.6,-0.2 –end-to-end–reorder; local parameters:–very-sensitive –L 20 –scoremin L,-0.6,-0.2 –end-to-end–reorder) through the HiC-Pro software[26] (Servant et al., 2015). Unmapped reads, non-uniquely mapped reads and PCR duplicates were filtered, uniquely aligned reads were paired, and replicates were merged (Table S1). Cis-contact matrices were assembled by binning paired reads into uniform 20 kb (human) or 10 kb (mouse) bins. After matrix assembly, poorly mapped regions were removed based on the mm9 and hg19 50-mer CRG Alignability tracks from ENCODE. The interactions of 50kb windows that uniquely aligned at a rate below 40% (mouse) and 50% (human) were set to NaN. Due to noticeably lower complexity in the human libraries, rows containing less than seven non-zero pixels within 200kb of the diagonal were completely removed during the human HiC analysis only. Matrices containing the remaining cis-contact counts were balanced using the Juicer implementation of the Knight Ruiz (KR) algorithm with default parameters[27]. The final bias factors were retained for subsequent loop calling (see next section). Balanced matrices were used for plotting (**Figure 1c, Extended Data 2**).

HiC Loop Calling

HiC interactions were tested for significance using methods first reported by Aiden and colleagues[8] with some minor alterations. To estimate the local background domain interaction frequency at each locus we utilized the donut expected model approach (described above,[8]) with parameters p=1, w=4 for the 20kb resolution human libraries and p=2, w=6 for the 10kb resolution mouse libraries. For each matrix entry the expected values were calculated using both the full donut window and just the lower-left region of the donut and the higher of the two was carried forward (i.e. expected = max(donut,lower-left))[2]. However, due to the extremely high on-diagonal counts we found this approach often over-estimated the expected background at short range interactions (less than 100kb). In order to accurately capture short range interactions, we modeled the on-diagonal (less than 100kb) background expected using only the upper-triangle region of the donut footprint. Expected contact matrices were then 'deconvoluted' back to discrete counts using the bias factors generated during KR balancing (see previous section)[8]. Each entry in the cis-contact matrix (pre-balancing) was tested for significance using a poisson distribution parameterized by its corresponding deconvoluted expected value[8]. Resulting p-values were corrected for multiple testing using the Benjamini-Hochberg procedure. In order for an interaction to be called as significantly enriched above background, it was required to pass 3 thresholds: 1) a q-value threshold ($q<0.01$ human, $q<0.025$ mouse);

2) a balanced-count threshold (count>10 human, count>20 mouse); 3) a distance threshold (distance>60 kb human, distance > 40 kb mouse). Matrix entries passing these thresholds were clustered by adjacency into loops; loops made up of fewer than 2 (human) or 3 (mouse) constituent matrix entries (interactions) were removed from further analysis.

Activity-Dependent Loop Classification and Gene Expression Analysis

Both 5C and mouse HiC loops were classified by the presence of enhancers at their anchors into mutually exclusive loop classes. 5C loops (Bic-only, TTX-only, constitutive) were classified using a specific order of intersection: loops were classified as containing a Bic-specific (activity-induced) enhancer (Classes 1+2, **Figures 3d,e** green) if a Bic-specific (activity-induced) enhancer fell at (at least) one of its loop anchors. Of the loops that did not intersect a Bic-specific or constitutive enhancer, the loop was then Class 3 if a TTX-specific (activity-decommissioned) enhancer intersected a loop anchor (Class 3, **Figures 3d,e**, purple). If the loop's anchors intersected no enhancers but did intersect a promoter (defined as +/- 2kb surrounding RefSeq TSS's downloaded from UCSC genome browser) it was classified as a 'TSS loop' (**Figure 3d**, orange). The remaining loops of each class (Bic-only, TTX-only, constitutive loops) were 'Unclassified' because they did not intersect a queried epigenetic feature. The three classes highlighted in subsequent analyses (**Figures 3d-j**) were Bic-specific enhancers in Bic-only loops (Class 1), Bic-specific enhancers in constitutive loops (Class 2), and TTX-specific enhancers in constitutive loops (Class 3). The average observed/expected signal for each looping cluster in each looping class was calculated (**Figure 3f**). The promoter (+/- 2kb of TSS) of each RefSeq transcript was then tested for whether it overlapped a loop anchor of each class. If multiple transcripts of the same gene shared (had overlapping) promoters, only the transcript with the maximum expression (TPM) across the Bic and TTX conditions was considered. Additionally, genes were not considered if they fell within 200kb of the edges of our 5C regions because we could not accurately capture their looping profiles. Those transcripts linked to promoters that fell at the base of each loop class were analyzed for Bic/TTX expression upregulation (**Figure 3g**) and Class 1 genes were analyzed for their gene ontology (GO) enrichment (**Figure 3j**).

Genes at the base of genome-wide mouse cortical neuron (CN) HiC loops (original data from Bonev+ 2017) were similarly classified into mutually exclusive groups based on the enhancers to which they looped (**Figures 3h-j**). HiC loops were first classified based on enhancers that intersected each anchor; Class 2 anchors contain activity-induced enhancers with no activity-decommissioned enhancers, Class 3 anchors contain activity-decommissioned enhancers with no activity-induced enhancers. If an enhancer class overlapped the upstream anchor, the downstream anchor was queried for intersection with promoters. If multiple transcripts of the same gene had promoters that overlapped the same anchor, only the transcript with the highest average expression across the Bic and TTX conditions was considered.

Gene ontology enrichment was performed using WebGestalt[28] (http://www.webgestalt.org/) with the following settings: Organism of interest = mmusculus; Method of interest = overrepresentation enrichment, Functional database = geneontology, biological_process_noRedun. refSeq mRNA IDs were uploaded for each set of classified genes. The genome_protein-coding set was used as the reference set for genome-wide HiC gene classes; all genes that fell within our 5C regions were used as the reference set for 5C gene class enrichment. The enrichment ratios and $-\log_{10}$(BH FDR) values for all GO terms with an FDR < 0.05 were plotted (**Figure 3j, Extended Data 7e**).

Rapid/Delayed Immediate Early Gene and Secondary Response Gene Analysis

We analyzed rapid primary response genes (rIEG), delayed primary response genes (dIEG), and secondary response genes (SRG) by downloading Supplemental Table 5 from Tyssowski et al. 2018[29]. Genes were removed from each class if their promoter (upstream 10kb from TSS) did not overlap an H3K27ac peak called in the Bic condition or the gene (plus 10kb promoter) did not intersect the anchor of a mouse HiC CN looping interaction. The number of loops each gene (plus 10kb promoter) intersected was recorded (**Figure 4k**). Additionally, the distance of each loop was calculated as the difference between the center point of the two anchors (**Figure 4l**). For each loop in which an rIEG, dIEG, or SRG gene was at one anchor, the other anchor was tested for an intersection with Bic-specific enhancers. The number of loop anchor paired with each gene that intersected a Bic-specific enhancer were tallied (genes which did not loop to any Bic-specific enhancers were not considered) (**Extended Data 8c**). Representative boxplots depict: center line, median; box limits, upper and lower quartiles; whiskers, 1.5x interquartile range; points, outliers. Expression timing of Bdnf, Arc, and Fos were calculated using Supplemental Table 2 from Tyssowski et al. 2018[29]. Each count was normalized to the maximum count for that gene across the 4 time points. The mean normalized count at each time point was plotted along with 95% confidence intervals (**Figure 4a**).

Disease-Associated GWAS Single Nucleotide Variant (SNV) Enrichment

Common variants associated with neurodevelopmental diseases were analyzed from the following sources:

- Schizophrenia: Schizophrenia Working Group of the Psychiatric Genomics, *Nature*, 2014 [30]
    - P-value $\leq 5 \times 10{-}8$, Table S2 from the referenced paper
- Autism Spectrum Disorder: Autism Spectrum Disorders Working Group of The Psychiatric Genomics, *Mol Autism*, 2017 [31] (European population)
    - P-value < 10-4, Additional File S3 from the referenced paper

Disease-associated SNVs (daSVs) that fell within exons or gene promoters (2 kb upstream of TSS) were discarded from analysis. RsIDs for each disease set were uploaded to SNPSNAP[32] in order to generate 10,000 matched 'background' SNVs for each daSNV. daSNVs were matched according the 1000Genomes Phase 3 European dataset at an LD distance cut-off of r^2=0.7 and LD buddies at r^2=0.7. daSNVs that could not be background matched using SNPSNAP were discarded. Genome-wide linkage disequilibrium (LD) r^2 values for SNV pairs were downloaded from the SNIPA tool[33]. For each daSNV and background SNV, an LD block was identified as the set of nucleotides for which the SNV in question had an r^2>0.7. Background LD blocks that overlapped each other or a disease-associated block were removed. The size of each LD block, disease and background, was calculated as the number of constituent SNVs. For each daSNV, 5 background SNVs with the same size LD block were selected. If fewer than 5 background LD blocks of the exact same size existed, background LD blocks of size one greater and one smaller than the disease-associated LD block in question were included in the set of 5 size-matched background LD blocks. The size of included background blocks was iteratively increased by one until 5 size-matched background LD blocks could be selected. If fewer than 5 background LD blocks had a size within 10 of the disease-associated block, successful background matching could not occur and the process was stopped. For example, for a daSNV with an LD block of size 75, background SNVs with LD blocks of sizes 65-85 could be matched, with preference given to those of size 75, then 74/76, and so on. Disease-associated SNVs which could not be successfully matched to 5 background LD blocks were removed from further analysis. (Note: For schizophrenia-associated SNVs, the number of size-matched LD blocks was decreased to 4 per daSNV.) If more than 5 background LD blocks were equally able to be matched to a given daSNV, 5 were

randomly chosen. Due to this randomness in the algorithm, 100 different sets of background size-matched SNVs were chosen for each daSNV (note 100 datapoints in **Figure 6b**, one per background set).

LD blocks (disease and background) were tested for their presence at loop anchors in the following manner. Loops were called on germinal zone (GZ) and cortical plate (CP) fetal brain tissue HiC data from Won et al. 2016[24] (see HiC processing steps above). CP and GZ loops were then merged to create a master set of 24,544 loops spanning the two brain tissues. Additionally, 25,722 'background loops' were identified as those HiC contact matrix entries which had a p-value > 0.99 and an interaction frequency count > 0 in both CP and GZ datasets. Background loops were confirmed to display the same loop distances and loop sizes as the real loop set. Bic-specific, TTX-specific, and constitutive enhancers were lifted over to the hg19 genome build using the liftOver tool on the UCSC genome browser with default parameters. Fetal brain loops were classified by enhancer presence at its anchor(s) in the same way mouse cortical neuron HiC loops were (see above). Queried LD blocks were then classified based on their presence at loop anchors: if any SNV in the LD block overlapped a loop anchor that was shared by a TTX-specific enhancer and not a Bic-specific enhancer, the LD block was considered a Class 3 variant; if any SNV in the LD block overlapped a loop anchor that was shared by a Bic-specific enhancer and not a TTX-specific enhancer, the LD block was considered a Class 2 variant. LD blocks had to fall at the same anchor as the enhancer to be classified. Finally, those LD blocks that did not overlap a classified loop anchor were tested for their presence at the anchor of a background loop. For each class, enrichment was calculated using Fisher's Exact Test with the following contingency table:
[[disease-associated blocks in loop of class X, background blocks in loop of class X],
[disease-associated blocks in background loops, background blocks in background loops]].
The resulting odds ratios were recorded for each of the 100 background size-matched SNV sets and plotted (**Figure 6b**) with the median p-value of the 100 tests.

LD Score Regression

To assess the polygenic enrichments of GWAS datasets listed above within looping classes, we applied LD score regression[34, 35]. LDSR was run on European subset of summary statistics from each GWAS. We used precomputed LD scores based on the European ancestry samples of the 1000 Genomes Project[36, 37] restricted to HapMap3 SNVs and generated partitioned LD scores for each looping class. All default LDSR parameters were used. LDSC version 1.0.0 was used (https://github.com/bulik/ldsc).

We conducted enrichment analyses of the heritability for SNVs located in each looping class. We regressed the $\chi 2$ from the GWAS summary statistics on to looping class-specific LD scores, with baseline scores (original 53 annotation model), regression weights and allele frequencies based on European ancestry 1000 Genome Project data. The enrichment of a looping class was defined as the proportion of SNV heritability in the category divided by the proportion of SNVs in that category; we report enrichment values and statistical significance of this enrichment as p-values (**Figure 6c**).

Disease-Associated Gene Expression

For each loop that was found to have a disease associated LD block and classified enhancer at one anchor (see previous section), the other anchor of the same loop was tested for intersection with promoters (+/- 2kb from TSS of human RefSeq database, downloaded from UCSC genome browser). To identify as many target genes as possible, disease-associated LD blocks that could not be size-matched in the previous section *were* included here because no enrichment against background SNVs was being calculated (however, those SNVs that were not in the 1000Genomes database and therefore could not be assigned LD blocks or

matched in SNPSNAP were still excluded, along with all daSNVs that overlapped exons and promoters). Promoters that colocalized on the other side of classified loops are annotated in **TableS19** and **Figure 6d**. Human gene symbols were matched to mouse homologs using the Jackson labs complete list of human and mouse homologs (http://www.informatics.jax.org/downloads/reports/HOM_MouseHumanSequence.rpt). Mouse homologs of classified genes that fell in loops across from disease-associated LD blocks could then be stratified by their Bic/TTX expression (TPM) fold change and plotted (**Figure 6d**).

Statistics

For linear regression modeling (**Figure 2f-l**), the ordinary least squares package from statsmodels (https://www.statsmodels.org/dev/examples/notebooks/generated/ols.html) was used to generate and plot best fit lines with 95% confidence intervals (**Figure 2f-j, Extended Data 6b-c**). The best fit coefficients, their t-test p-values and standard error estimates were plotted as barplots (**Fig. 2l, Extended Data 6e**). Gene expression differences across looping classes (**Fig. 3f-h**) were tested for significance using the scipy Wilcoxon test (https://docs.scipy.org/doc/scipy/reference/generated/scipy.stats.wilcoxon.html). Loop complexity differences across gene class (**Fig. 4k-l**) were tested for significance using the scipy Mann-Whitney U test (https://docs.scipy.org/doc/scipy/reference/generated/scipy.stats.mannwhitneyu.html#scipy.stats.mannwhitneyu). SNV overlap of classified loop anchors (**Fig. 6b**) was tested for significance using Fisher's Exact test. No statistical methods were used to pre-determine sample sizes but our sample sizes are similar to those reported in previous publications[2, 8]. Treatment conditions were evenly distributed across culture batches and treatments were randomly assigned to culture dishes within each batch. Data collection and analysis were not performed blind to the conditions of the experiments. No animals or data points were excluded from the analyses.

Supplemental References

1. Shepherd, J.D. et al. Arc/Arg3.1 mediates homeostatic synaptic scaling of AMPA receptors. *Neuron* **52**, 475-484 (2006).
2. Beagan, J.A. et al. YY1 and CTCF orchestrate a 3D chromatin looping switch during early neural lineage commitment. *Genome Res* **27**, 1139-1152 (2017).
3. Beagan, J.A. et al. Local Genome Topology Can Exhibit an Incompletely Rewired 3D-Folding State during Somatic Cell Reprogramming. *Cell Stem Cell* **18**, 611-624 (2016).
4. Langmead, B. Aligning short sequencing reads with Bowtie. *Curr Protoc Bioinformatics* **Chapter 11**, Unit 11 17 (2010).
5. Zhang, Y. et al. Model-based analysis of ChIP-Seq (MACS). *Genome Biol* **9**, R137 (2008).
6. Ramirez, F. et al. deepTools2: a next generation web server for deep-sequencing data analysis. *Nucleic Acids Res* **44**, W160-165 (2016).
7. Kim, J.H. et al. 5C-ID: Increased resolution Chromosome-Conformation-Capture-Carbon-Copy with in situ 3C and double alternating primer design. *Methods* **142**, 39-46 (2018).
8. Rao, S.S. et al. A 3D map of the human genome at kilobase resolution reveals principles of chromatin looping. *Cell* **159**, 1665-1680 (2014).
9. Sun, J.H. et al. Disease-Associated Short Tandem Repeats Co-localize with Chromatin Domain Boundaries. *Cell* **175**, 224-238 e215 (2018).
10. Hnisz, D. et al. Activation of proto-oncogenes by disruption of chromosome neighborhoods. *Science* **351**, 1454-1458 (2016).
11. Sun, J.H. et al. Disease-Associated Short Tandem Repeats Co-localize with Chromatin Domain Boundaries. *Cell* (2018).
12. Kim, J.H. et al. LADL: light-activated dynamic looping for endogenous gene expression control. *Nat Methods* **16**, 633-639 (2019).
13. Lajoie, B.R., van Berkum, N.L., Sanyal, A. & Dekker, J. My5C: web tools for chromosome conformation capture studies. *Nat Methods* **6**, 690-691 (2009).
14. Dixon, J.R. et al. Topological domains in mammalian genomes identified by analysis of chromatin interactions. *Nature* **485**, 376-380 (2012).
15. Gilgenast, T.G. & Phillips-Cremins, J.E. Systematic Evaluation of Statistical Methods for Identifying Looping Interactions in 5C Data. *Cell Syst* **8**, 197-211 e113 (2019).
16. Imakaev, M. et al. Iterative correction of Hi-C data reveals hallmarks of chromosome organization. *Nat Methods* **9**, 999-1003 (2012).
17. Phillips-Cremins, J.E. et al. Architectural protein subclasses shape 3D organization of genomes during lineage commitment. *Cell* **153**, 1281-1295 (2013).
18. Fernandez, L.R., Gilgenast, T.G. & Phillips-Cremins, J.E. 3DeFDR: Identifying cell type-specific looping interactions with empirical false discovery rate guided thresholding. *bioRxiv*, 501056 (2018).
19. Patro, R., Duggal, G., Love, M.I., Irizarry, R.A. & Kingsford, C. Salmon provides fast and bias-aware quantification of transcript expression. *Nat Methods* **14**, 417-419 (2017).
20. Pimentel, H., Bray, N.L., Puente, S., Melsted, P. & Pachter, L. Differential analysis of RNA-seq incorporating quantification uncertainty. *Nat Methods* **14**, 687-690 (2017).
21. Dobin, A. et al. STAR: ultrafast universal RNA-seq aligner. *Bioinformatics* **29**, 15-21 (2013).
22. Fulco, C.P. et al. Activity-by-Contact model of enhancer specificity from thousands of CRISPR perturbations. *bioRxiv*, 529990 (2019).
23. Bonev, B. et al. Multiscale 3D Genome Rewiring during Mouse Neural Development. *Cell* **171**, 557-572 e524 (2017).
24. Won, H. et al. Chromosome conformation elucidates regulatory relationships in developing human brain. *Nature* **538**, 523-527 (2016).

25. Langmead, B. & Salzberg, S.L. Fast gapped-read alignment with Bowtie 2. *Nat Methods* **9**, 357-359 (2012).
26. Servant, N. et al. HiC-Pro: an optimized and flexible pipeline for Hi-C data processing. *Genome Biol* **16**, 259 (2015).
27. Durand, N.C. et al. Juicer Provides a One-Click System for Analyzing Loop-Resolution Hi-C Experiments. *Cell Syst* **3**, 95-98 (2016).
28. Wang, J., Vasaikar, S., Shi, Z., Greer, M. & Zhang, B. WebGestalt 2017: a more comprehensive, powerful, flexible and interactive gene set enrichment analysis toolkit. *Nucleic Acids Res* **45**, W130-W137 (2017).
29. Tyssowski, K.M. et al. Different Neuronal Activity Patterns Induce Different Gene Expression Programs. *Neuron* **98**, 530-546 e511 (2018).
30. Schizophrenia Working Group of the Psychiatric Genomics, C. Biological insights from 108 schizophrenia-associated genetic loci. *Nature* **511**, 421-427 (2014).
31. Autism Spectrum Disorders Working Group of The Psychiatric Genomics, C. Meta-analysis of GWAS of over 16,000 individuals with autism spectrum disorder highlights a novel locus at 10q24.32 and a significant overlap with schizophrenia. *Mol Autism* **8**, 21 (2017).
32. Pers, T.H., Timshel, P. & Hirschhorn, J.N. SNPsnap: a Web-based tool for identification and annotation of matched SNPs. *Bioinformatics* **31**, 418-420 (2015).
33. Arnold, M., Raffler, J., Pfeufer, A., Suhre, K. & Kastenmuller, G. SNiPA: an interactive, genetic variant-centered annotation browser. *Bioinformatics* **31**, 1334-1336 (2015).
34. Bulik-Sullivan, B.K. et al. LD Score regression distinguishes confounding from polygenicity in genome-wide association studies. *Nat Genet* **47**, 291-295 (2015).
35. Finucane, H.K. et al. Partitioning heritability by functional annotation using genome-wide association summary statistics. *Nat Genet* **47**, 1228-1235 (2015).
36. International HapMap, C. et al. Integrating common and rare genetic variation in diverse human populations. *Nature* **467**, 52-58 (2010).
37. Genomes Project, C. et al. An integrated map of genetic variation from 1,092 human genomes. *Nature* **491**, 56-65 (2012).

Extended Data Figures

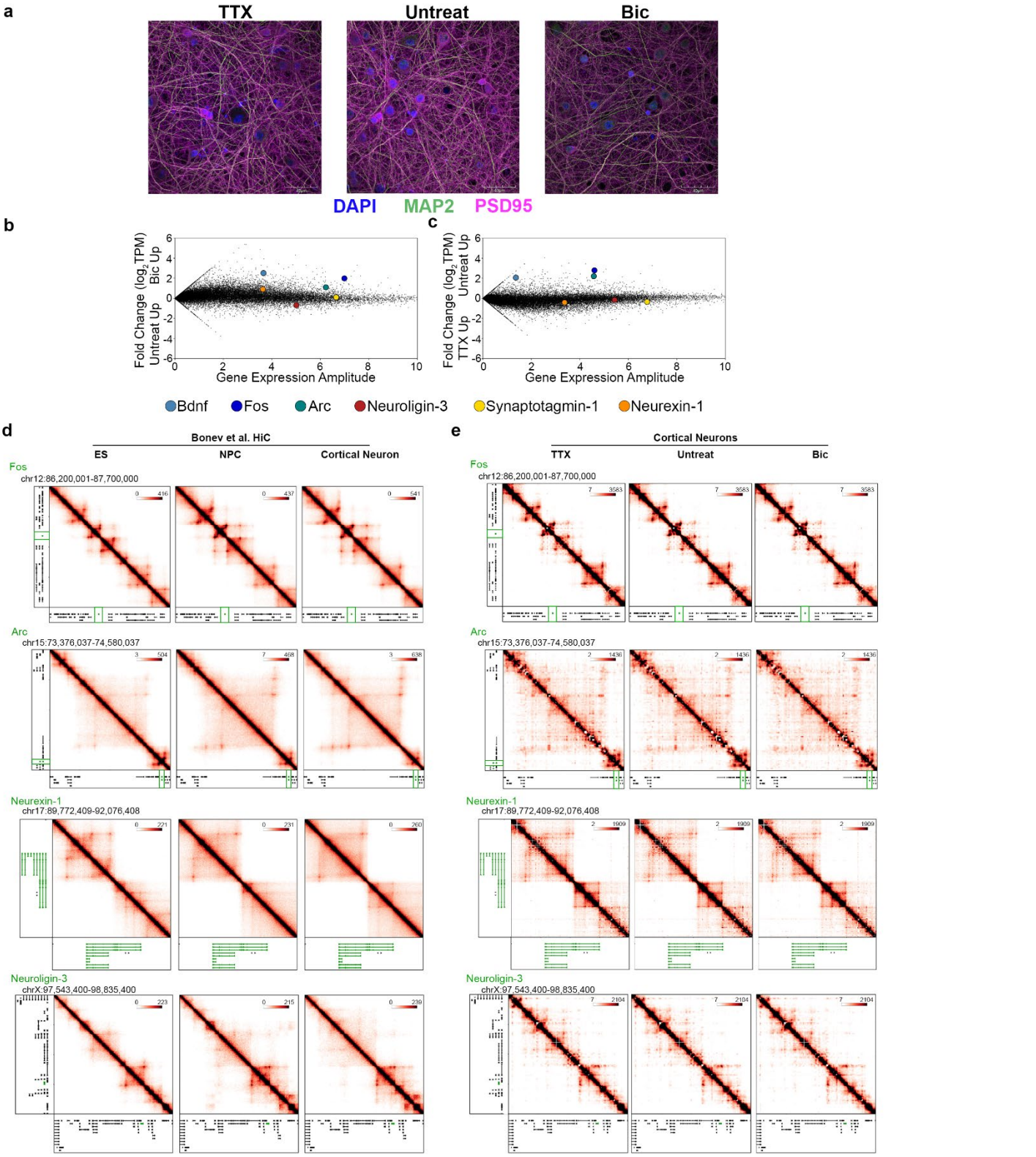

Extended Data 1 (Associated with Figure 1). Mapping genome folding across neural activity states. **(a)** Representative immunofluorescence images of DAPI (blue), MAP2 (green), PSD95 (magenta) signal across conditions. Results were consistent across 2 culture batches, 4 total 5C replicates, 3 RNA-seq replicates, and H3K27ac ChIP replicate analyzed. **(b-c)** Fold change vs amplitude plots of RNA-seq data comparing the Bic vs Untreat conditions (b) and TTX vs Untreat conditions (c). **(d)** Interaction frequency heatmaps of 1-3 Mb regions surrounding the Fos, Arc, Neurexin-1, and Neuroligin-3 genes (labeled in green) across embryonic stem (ES) cells, neural progenitor cells (NPCs), and cortical neurons (CNs) (data analyzed from Bonev+ 2017). **(e)** Interaction frequency heatmaps of the regions presented in (a) across tetrodotoxin-treated (TTX), untreated, and bicuculline-treated (Bic) DIV16 cortical neurons.

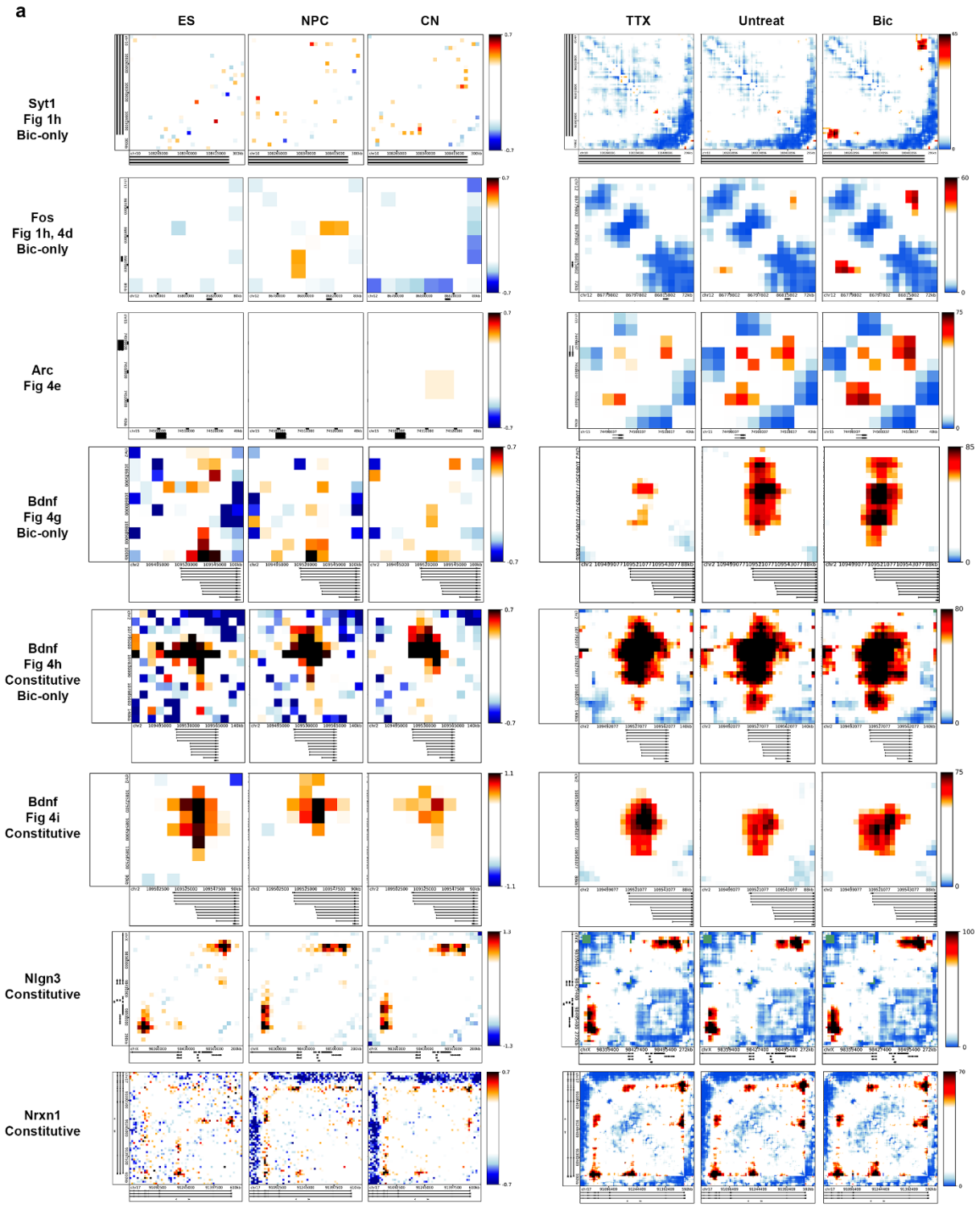

Extended Data 2 (Associated with Figure 1). Activity-induced loops are not present earlier in cortical neuron differentiation. (a) Zoom-in heatmaps of critical loops presented throughout the paper. From left to right the columns are Obs/Exp heatmaps of HiC (Bonev et al.) data from 1)

embryonic stem (ES) cells, 2) neural progenitor cells (NPC), 3) cortical neurons (CN), followed by 5C interaction score heatmaps across the 4) TTX, 5) untreated, and 6) BIC treated conditions. Genes of interest in each zoom window, Figure panels where same loop is further analyzed, and loop classification are listed on left.

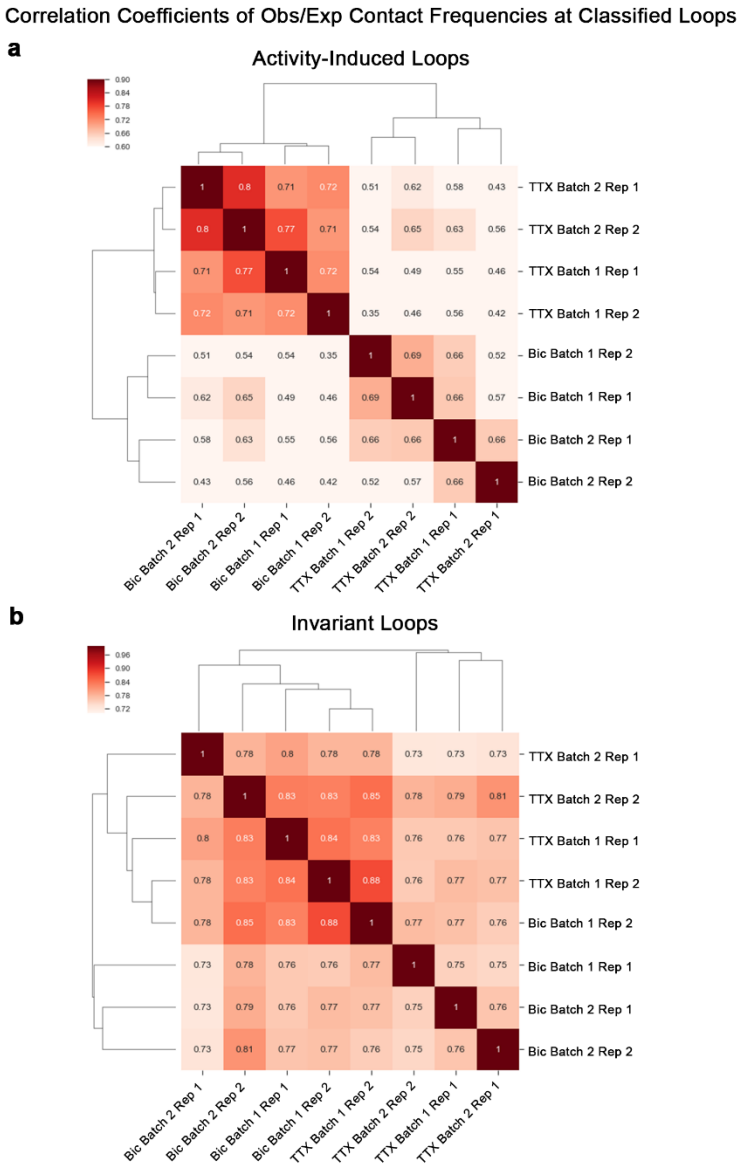

Extended Data 3 (Associated with Figure 1). 5C data correlations cluster by condition. (a-b) Pearson's correlation coefficients of background-normalized contact frequencies ("observed/expected") at activity-induced loops (a) and activity-invariant loops (b) across each pair of replicates. The N = 4 independent biological replicates for each condition were then hierarchically clustered based on correlation results.

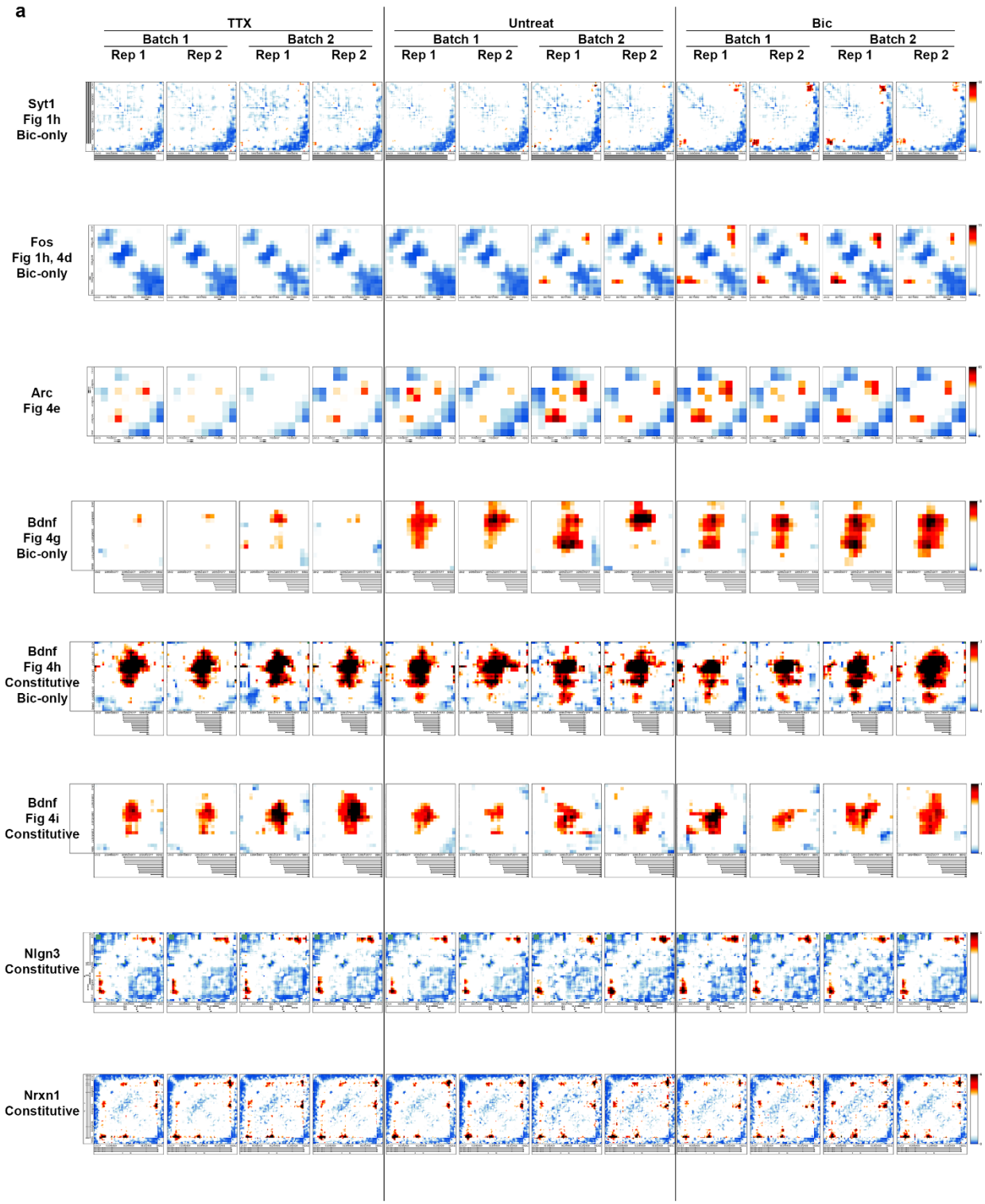

Extended Data 4 (Associated with Figure 1). Activity-induced and activity-invariant loops are reproducible across condition replicates. (a) Zoom-in interaction score heatmaps from each of the 12 5C replicates generated for critical loops presented throughout the paper. Genes of interest in each

zoom window, Figure panels where same loop is further analyzed, and loop classification are listed on left.

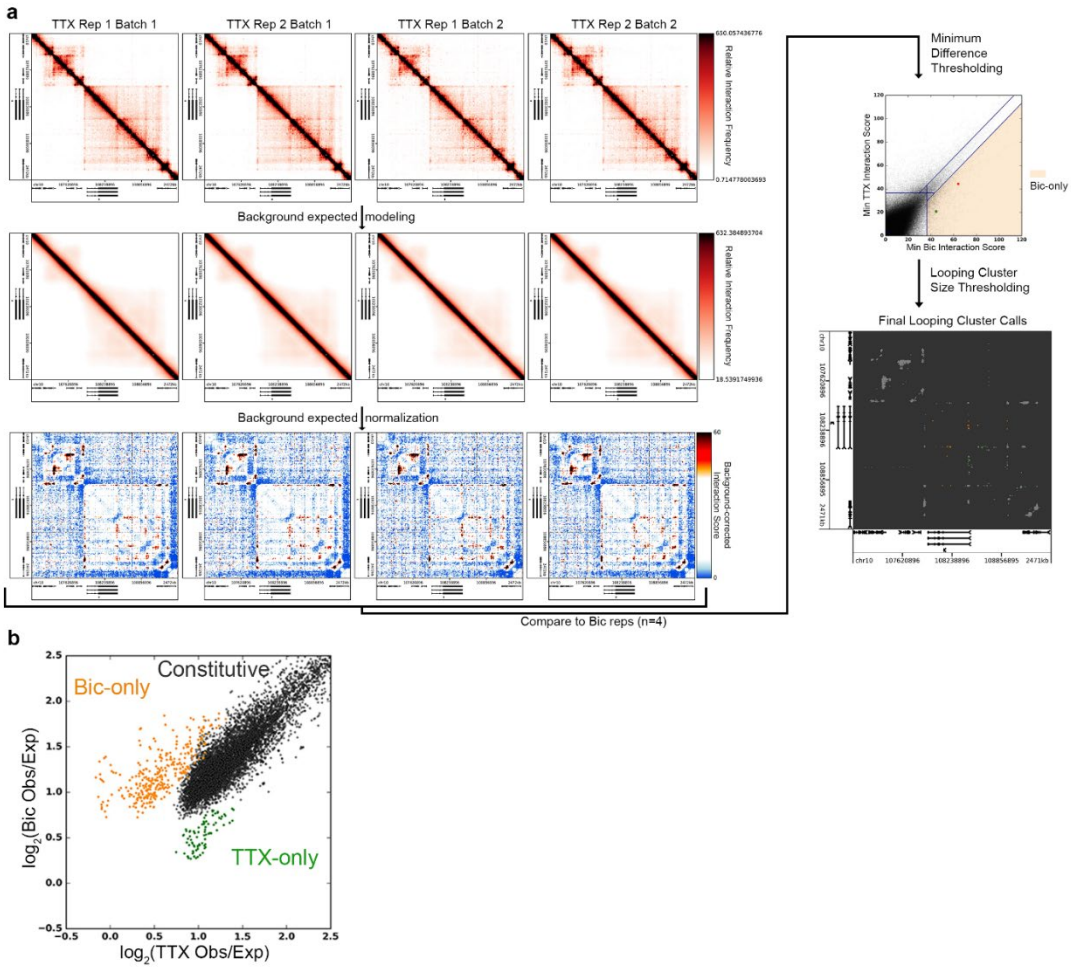

Extended Data 5 (Associated with Figure 1). Identifying dynamic looping across neural activity states. (a) Diagram of 5C processing pipeline used to call significant constitutive and dynamic loops (bottom right) starting from 5C interaction frequency counts for all pairs of 4 kb genomic bins within queried regions across 4 replicates (from two litter/culture batches) of each condition (top left). First the local domain background signal is quantified using a donut expected model (Rao+ 2014) and removed from the interaction frequency signal. Probabilistic modeling converts these expected-normalized interaction frequencies to an "interaction score" (bottom left). For a bin-bin pair to be classified as looping, its interaction score must fall above a given "significance threshold". For a looping bin-bin pair to be classified as "Bic-only" the minimum interaction score of the Bic replicates must exceed the maximum interaction score of the four TTX replicates by a given "difference threshold" (Supplemental Methods). Looping pixels not classified as Bic- or TTX-only are classified as constitutive (top right). Bin-bin pairs of the same class are then grouped into clusters if they are directly adjacent; clusters below a selected size threshold are removed from looping classification (bottom right). See Methods for more details. **(b)** Scatterplot of the background-normalized contact frequency ("Observed/Expected") counts of looping-classified pixels in TTX and Bic conditions.

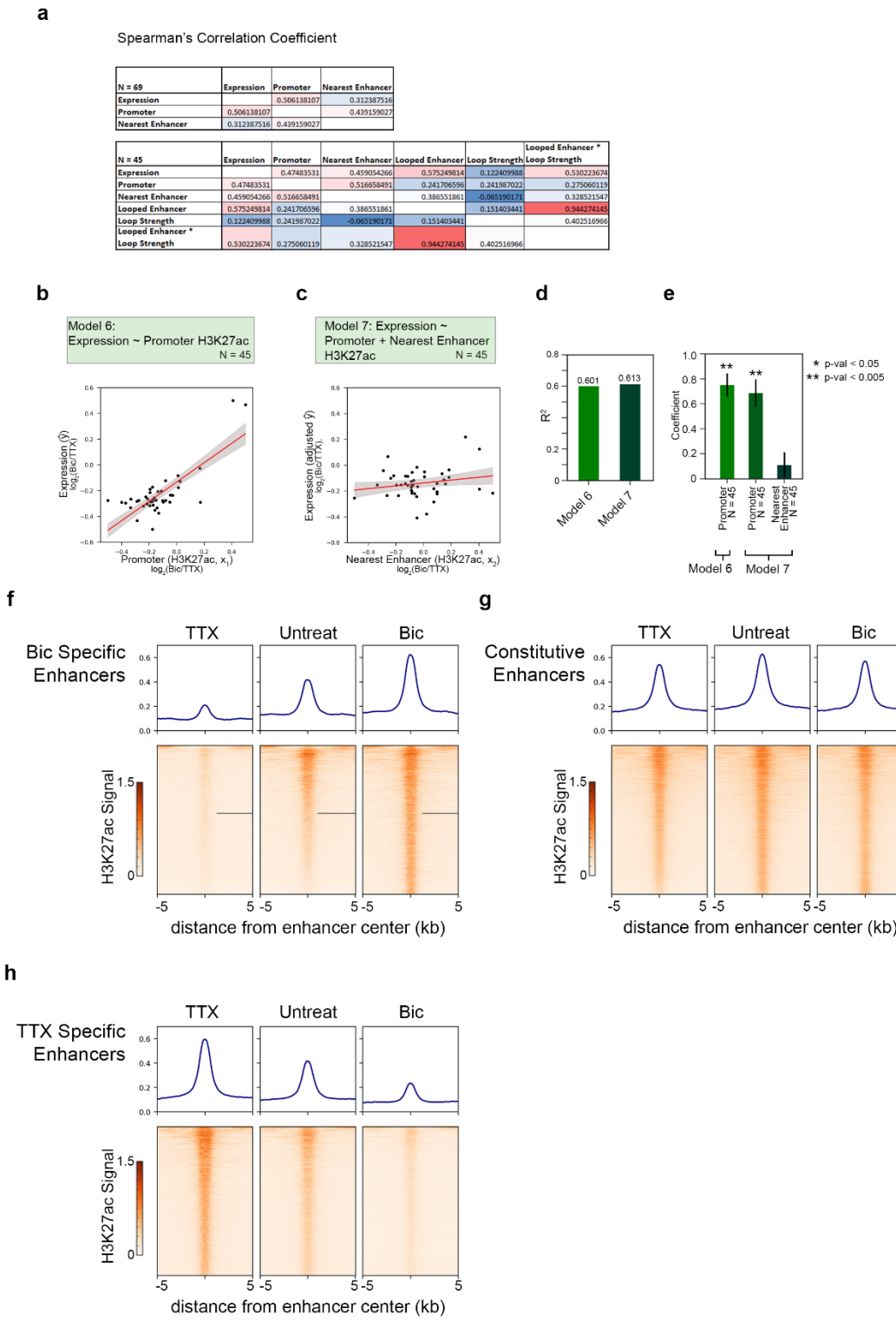

N = 69	Expression	Promoter	Nearest Enhancer
Expression		0.506138107	0.312387516
Promoter	0.506138107		0.439159027
Nearest Enhancer	0.312387516	0.439159027	

N = 45	Expression	Promoter	Nearest Enhancer	Looped Enhancer	Loop Strength	Looped Enhancer * Loop Strength
Expression		0.47483531	0.459054266	0.575249814	0.122409988	0.530223674
Promoter	0.47483531		0.516658491	0.241706596	0.241987022	0.275060119
Nearest Enhancer	0.459054266	0.516658491		0.386551861	-0.065190171	0.328521547
Looped Enhancer	0.575249814	0.241706596	0.386551861		0.151403441	0.944274145
Loop Strength	0.122409988	0.241987022	-0.065190171	0.151403441		0.402516966
Looped Enhancer * Loop Strength	0.530223674	0.275060119	0.328521547	0.944274145	0.402516966	

Extended Data 6 (Associated with Figure 2-3). Quantifying activity-dependent regulatory elements. (a) Spearman's correlation coefficients for terms included in models (Fig. 2f-i). **(b-c)** Results of promoter-only (b) and promoter plus nearest enhancer (c) models for only genes that form loops to

classified enhancers within 5C regions. N=45 genes analyzed. **(d)** R^2 values of models presented in (b-c). **(e)** Coefficients of each explanatory variable term in models presented in (b-c). t-statistic p-values and standard errors represented via stars and error bars, respectively. **(f-h)** Acetylation heatmaps, pileups of classified activity-induced (f), activity-decommissioned (g), invariant (h) enhancers.

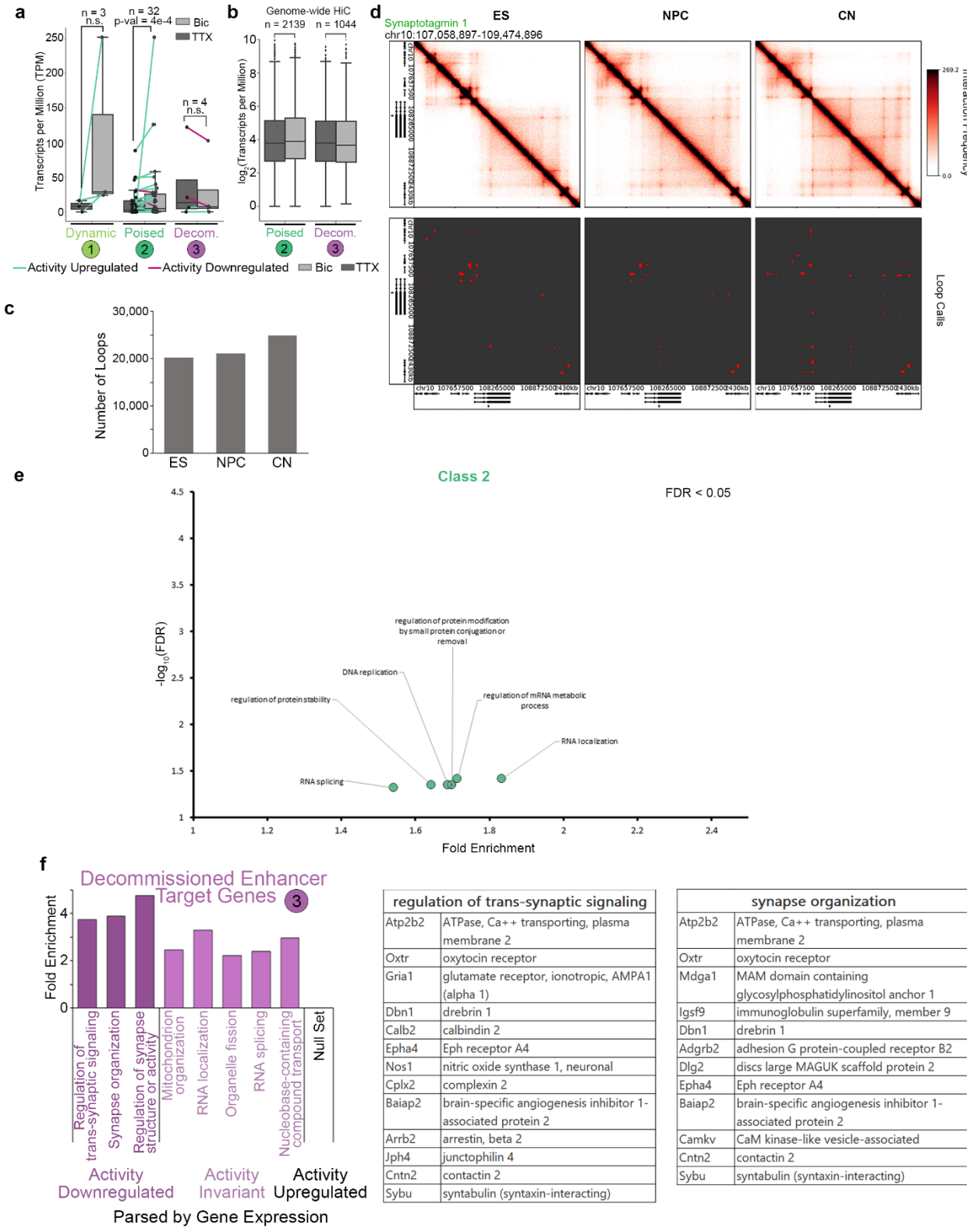

regulation of trans-synaptic signaling	
Atp2b2	ATPase, Ca++ transporting, plasma membrane 2
Oxtr	oxytocin receptor
Gria1	glutamate receptor, ionotropic, AMPA1 (alpha 1)
Dbn1	drebrin 1
Calb2	calbindin 2
Epha4	Eph receptor A4
Nos1	nitric oxide synthase 1, neuronal
Cplx2	complexin 2
Baiap2	brain-specific angiogenesis inhibitor 1-associated protein 2
Arrb2	arrestin, beta 2
Jph4	junctophilin 4
Cntn2	contactin 2
Sybu	syntabulin (syntaxin-interacting)

synapse organization	
Atp2b2	ATPase, Ca++ transporting, plasma membrane 2
Oxtr	oxytocin receptor
Mdga1	MAM domain containing glycosylphosphatidylinositol anchor 1
Igsf9	immunoglobulin superfamily, member 9
Dbn1	drebrin 1
Adgrb2	adhesion G protein-coupled receptor B2
Dlg2	discs large MAGUK scaffold protein 2
Epha4	Eph receptor A4
Baiap2	brain-specific angiogenesis inhibitor 1-associated protein 2
Camkv	CaM kinase-like vesicle-associated
Cntn2	contactin 2
Sybu	syntabulin (syntaxin-interacting)

Extended Data 7 (Associated with Figure 3). Assessing activity-dependent regulation using murine urine HiC (Bonev et al., 2017) loop calls. (a) Expression (TPM) of the transcripts whose promoters intersect each looping class. P-values presented calculated using two-tailed Wilcoxon

signed-rank test. **(b)** Expression (log_2(TPM)) of the genes whose promoters fall opposite activity-induced (class 2) and activity-decommissioned (class 3) enhancers in genome-wide cortical neuron loops, original data from Bonev et al. 2017. Number of genes in each class (a-b) listed as N = above boxes. Boxes in a-b range from lower to upper quartile with median line, whiskers extend to min/max data point within 1.5*interquartile range. (**c**) Number of loops called in HiC data obtained from embryonic stem cells (ES), neural progenitor cells (NPCs), and cortical neurons (CN) (Bonev et al. 2017). **(d)** Interaction frequency heatmaps (top) and thresholded loop calls (bottom) for a ~2.5 Mb region surrounding the *Syt1* gene. **(e)** The remaining gene ontology terms passing the FDR < 0.05 threshold for class 2 (a) which could not be presented in **Figure 3**. N = 2139 Class 2 genes, enrichment calculated using Webgestalt[28]. **(f)** (Left) Gene ontology enrichment ratios for class 3 genes parsed by expression into activity downregulated (Bic/TTX < 2/3), activity invariant (5/6 < Bic/TTX < 6/5), and activity upregulated (Bic/TTX > 3/2) groups. (Right) Genes found in the 'regulation of trans-synaptic signaling' and 'synapse organization' GO terms enriched in activity downregulated class 3 genes.

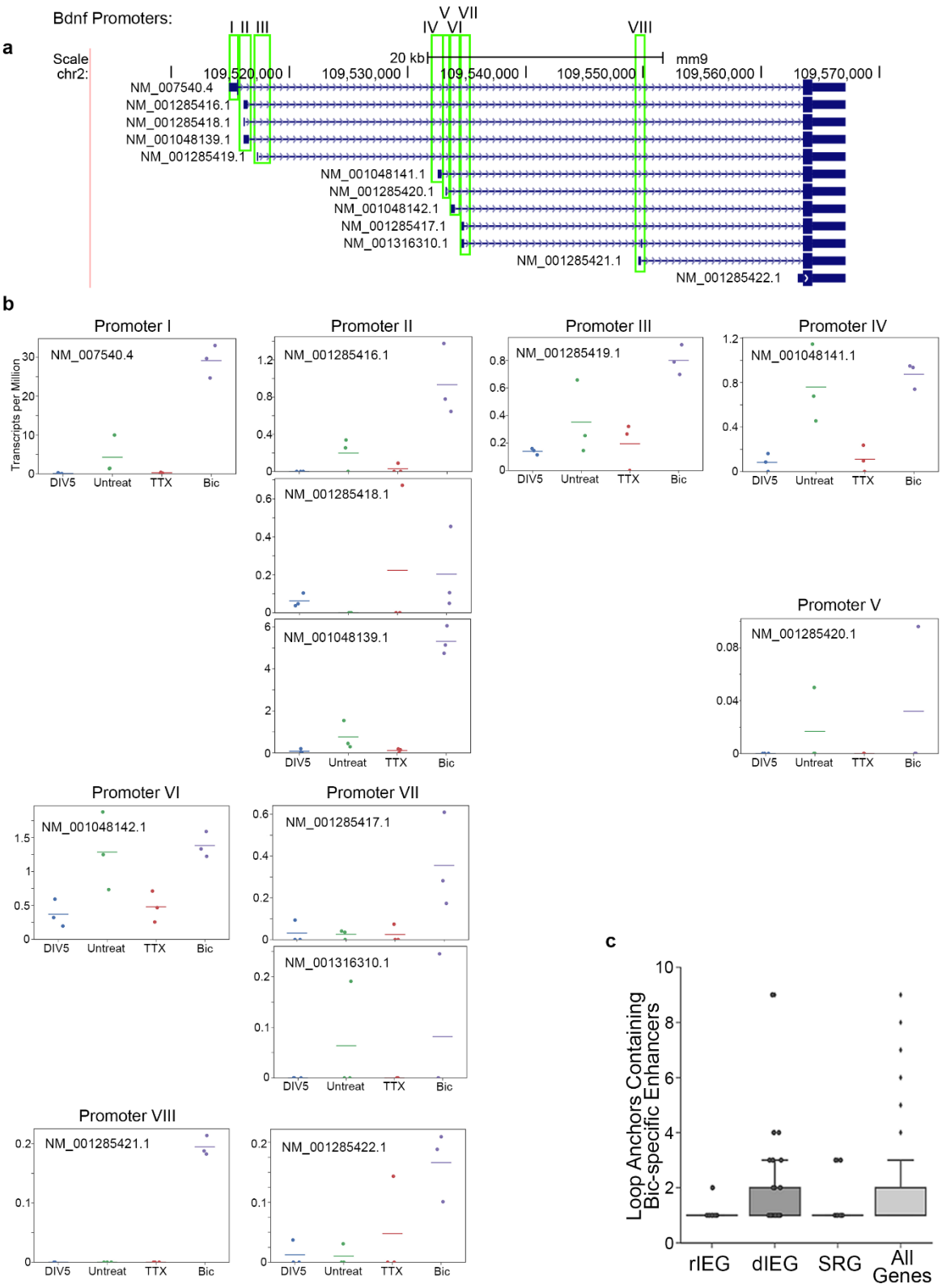

Extended Data 8 (Associated with Figure 4). Expression of *Bdnf* transcripts. (a) Depiction of the 12 RefSeq transcript isoforms of the *Bdnf* gene, above which we annotate the 8 promoters as in Hong et al., *Neuron*, 2008. **(b)** Expression strip plots of each *Bdnf* isoform, organized in columns by shared

promoter. N = 3, mean lines plotted. **(c)** Boxplots overlaid by strip plots of count of opposing looping anchors that contain an activity-dependent enhancer for rapid immediate early genes (rIEGs, as defined as rPRGs in Tyssowski et al. 2018), delayed IEGs (dIEGs, defined as dPRGs in Tyssowski et al. 2018), secondary response genes (SRGs, defined as SRGs in Tyssowski et al. 2018), and all genes. Boxes range from lower to upper quartile with median line, whiskers extend to min/max data point within 1.5*interquartile range.

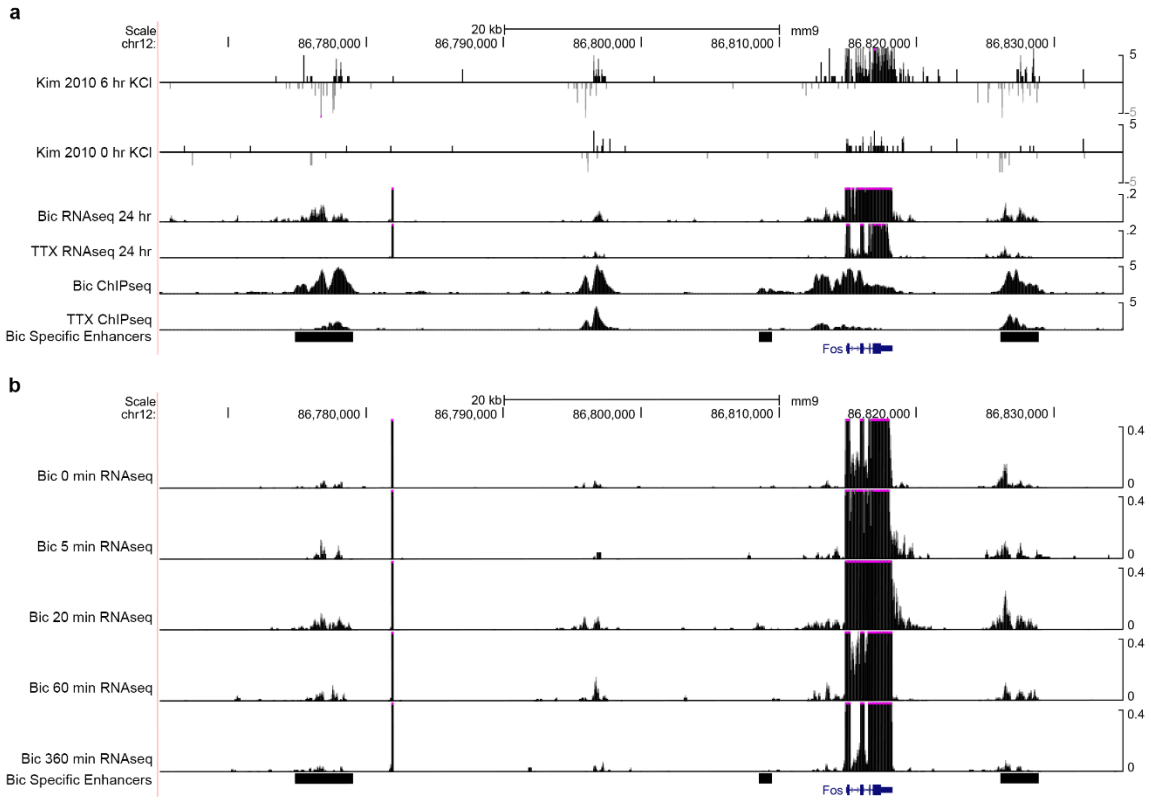

Extended Data 9 (Associated with Figure 5). Verification of the eRNA signature captures enhancer activity dynamics. (a) Genome browser view of ~50 kb window surrounding the *Fos* gene. Rows from top to bottom present: 1) RNA signal in active neurons from Kim et al. 2010, 2) RNA signal in inactive neurons from Kim et al. 2010, 3) RNA signal from neurons in the Bic condition, 4) RNA signal from neurons in the TTX condition, 5) H3K27ac ChIP-seq signal from neurons in the Bic condition, 6) H3K27ac ChIP-seq signal from neurons in the TTX condition. **(b)** RNA-seq signatures at enhancers near *Fos* across 0, 5, 20, 60, and 360 minutes of acute neuron activation.

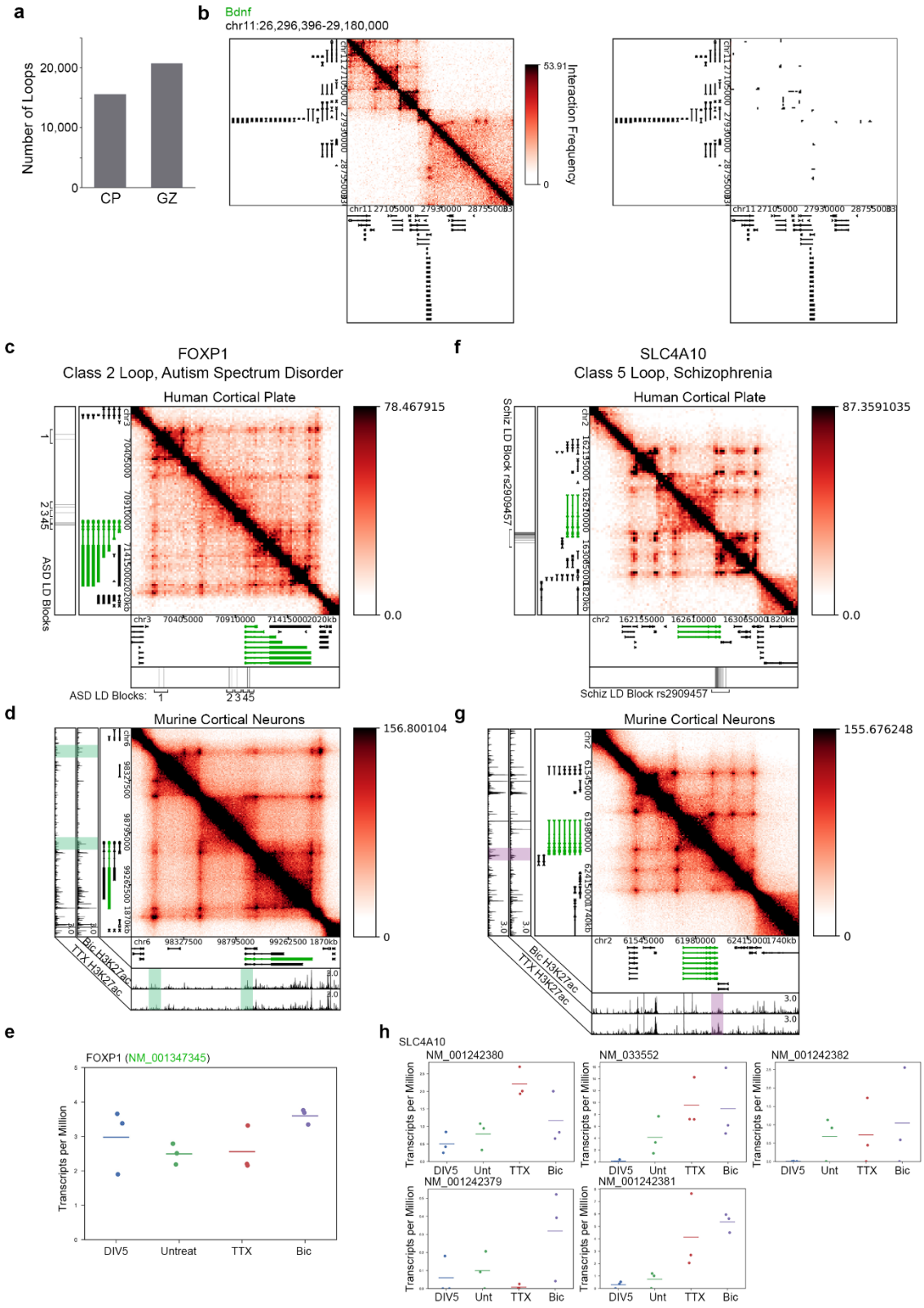
a
Number of Loops
20,000
10,000
0
CP
GZ
b
Bdnf
chr11:26,296,396-29,180,000
53.91
Interaction Frequency
0
c
FOXP1
Class 2 Loop, Autism Spectrum Disorder
Human Cortical Plate
78.467915
0.0
ASD LD Blocks
ASD LD Blocks:
f
SLC4A10
Class 5 Loop, Schizophrenia
Human Cortical Plate
87.3591035
0.0
Schiz LD Block rs2909457
d
Murine Cortical Neurons
156.800104
0
Bic H3K27ac
TTX H3K27ac
g
Murine Cortical Neurons
155.676248
0
e
FOXP1 (NM_001347345)
Transcripts per Million
DIV5
Untreat
TTX
Bic
h
SLC4A10
NM_001242380
NM_033552
NM_001242382
NM_001242379
NM_001242381
Transcripts per Million
DIV5
Unt
TTX
Bic

Extended Data 10 (Associated with Figure 6). *Foxp1* and *Slc4a10* fall opposite disease-Associated variants in conserved classified loops. (a) Number of loops called in HiC data obtained from human fetal cortical plate (CP) and germinal zone (GZ) tissue (Won et al. 2016). **(b)** Interaction frequency heatmap (left) and thresholded loop calls (right) of the 2.5 Mb region surrounding the *Bdnf* gene in human cortical plate (CP) fetal tissue. **(c-e)** Human (c) and mouse (d) interaction frequency heatmaps of a 2 Mb region surrounding the *Foxp1* gene. The expression of the looping Foxp1 isoform labeled in green in (d) is plotted in (e). **(f-h)** Human (f) and mouse (g) interaction frequency heatmaps of a <2 Mb region surrounding the *Slc4a10* gene (green), followed by expression of its 5 expressed isoforms (h). N = 3 RNA-seq replicates in (e,h), mean lines plotted.

Supplemental Tables

Table S1. Summary of new 5C datasets provided in this study

Condition	Rep	Cell Type	Primer Set*	5C Sequencing Run	Total Mapped Reads (Paired End 1)	Total Mapped Reads (Paired End 2)
Bic (DIV16)	1	Cortical Neuron	Activity	1	15629758	13994700
Bic (DIV16)	2	Cortical Neuron	Activity	1	17872216	16068115
Bic (DIV16)	3	Cortical Neuron	Activity	2	13358656	13182759
Bic (DIV16)	4	Cortical Neuron	Activity	2	12761525	12560359
Bic (DIV16)	1	Cortical Neuron	Synaptic	1	21489169	19378693
Bic (DIV16)	2	Cortical Neuron	Synaptic	1	14655973	13225858
Bic (DIV16)	3	Cortical Neuron	Synaptic	2	11258574	11108043
Bic (DIV16)	4	Cortical Neuron	Synaptic	2	10640297	10455808
TTX (DIV16)	1	Cortical Neuron	Activity	1	19957660	18061209
TTX (DIV16)	2	Cortical Neuron	Activity	1	19462095	17617327
TTX (DIV16)	3	Cortical Neuron	Activity	2	11475372	11280130
TTX (DIV16)	4	Cortical Neuron	Activity	2	11576011	11376399
TTX (DIV16)	1	Cortical Neuron	Synaptic	1	17730187	16044486
TTX (DIV16)	2	Cortical Neuron	Synaptic	1	22476694	20350478
TTX (DIV16)	3	Cortical Neuron	Synaptic	2	12489964	12229149
TTX (DIV16)	4	Cortical Neuron	Synaptic	2	12474307	12266865
Untreat (DIV16)	1	Cortical Neuron	Activity	1	20574076	18647762
Untreat (DIV16)	2	Cortical Neuron	Activity	1	19880857	17961279
Untreat (DIV16)	3	Cortical Neuron	Activity	2	10041836	9843702
Untreat (DIV16)	4	Cortical Neuron	Activity	2	10897728	10658216
Untreat (DIV16)	1	Cortical Neuron	Synaptic	1	24964591	22576821
Untreat (DIV16)	2	Cortical Neuron	Synaptic	1	17861704	16068258
Untreat (DIV16)	3	Cortical Neuron	Synaptic	2	11232157	11041243
Untreat (DIV16)	4	Cortical Neuron	Synaptic	2	10945734	10777809

*5C Primer Sets:
Activity = BDNF, FOS, ARC
Synaptic = NRXN1, SYT1, NLGN3

Table S2 – Summary of new RNA-seq datasets provided in this study

Condition	Rep Name	Sequenced Reads	Mapped Reads (RefSeq Transcriptome)
DIV5	DIV5_2-2-17_Rep1	66596616	42931843
Div5	DIV5_2-2-17_Rep2	66127710	43785136
Div5	DIV5_2-5-17_Rep2	74490452	45382360
Untreated	DIV16_Untreat_2-13-17_Rep1	76292600	45728980
Untreated	DIV16_Untreat_2-13-17_Rep2	70313996	43709559
Untreated	DIV16_Untreat_2-16-17_Rep2	73031884	41965444
TTX	DIV16_TTX_2-13-17_Rep1	67865345	42933935
TTX	DIV16_TTX_2-13-17_Rep2	71808738	43452817
TTX	DIV16_TTX_2-16-17_Rep1	80579287	54155741
Bic	DIV16_Bicuc_2-13-17_Rep1	71158871	46802769
Bic	DIV16_Bicuc_2-13-17_Rep2	70726507	43333176
Bic	DIV16_Bicuc_2-16-17_Rep2	76301581	46085188

Table S3 –Transcripts per million (TPM) counts across DIV and activation time points for RefSeq transcriptome

Provided in separate spreadsheet.

Table S4 – Results of the Sleuth Wald test for differential expression

Provided in separate spreadsheet.

Table S5 – Summary of previously published HiC datasets analyzed

Tissue/Cell Type	Rep	Total Mapped Reads (Paired End 1)	Total Mapped Reads (Paired End 2)	Total Valid Pairs	Assembly	GEO Sample ID	Reference
ES	1	2456874859	2410167937	1694547628	mm9	GSM2533818	(Bonev et al. 2017)
ES	2	1263130596	1228304467	874261374	mm9	GSM2533819	(Bonev et al. 2017)
ES	3	2673778757	2640856932	1861707555	mm9	GSM2533820	(Bonev et al. 2017)
ES	4	508261688	499843892	355266330	mm9	GSM2533821	(Bonev et al. 2017)
ES	**merged**	**6902045900**	**6779173228**	**4785782887**			
NPC	1	1224587101	1216240550	850812082	mm9	GSM2533822	(Bonev et al. 2017)
NPC	2	2076449282	2073685785	1425496094	mm9	GSM2533823	(Bonev et al. 2017)
NPC	3	1443846007	1437360743	967787722	mm9	GSM2533824	(Bonev et al. 2017)
NPC	4	3538265465	3534220365	2465796658	mm9	GSM2533825	(Bonev et al. 2017)

NPC	**merged**	**8283147855**	**8261507443**	**5709892556**			
Cortical Neuron	1	742260464	738703350	510995484	mm9	GSM2533826	(Bonev et al. 2017)
Cortical Neuron	2	741509478	736455469	515304241	mm9	GSM2533827	(Bonev et al. 2017)
Cortical Neuron	3	1050785183	1052901789	732518157	mm9	GSM2533828	(Bonev et al. 2017)
Cortical Neuron	4	1668657503	1662949431	1163551034	mm9	GSM2533829	(Bonev et al. 2017)
Cortical Neuron	5	2324686938	2092692067	1430515014	mm9	GSM2533830	(Bonev et al. 2017)
Cortical Neuron	6	1797395887	1792866442	1237396926	mm9	GSM2533831	(Bonev et al. 2017)
Cortical Neuron	**merged**	**8325295453**	**8076568548**	**5590280856**			
Cortical Plate	1	680901460	669828525	477401617	hg19	GSM2054564	(Won et al. 2016)
Cortical Plate	2	668075261	655925822	479063672	hg19	GSM2054565	(Won et al. 2016)
Cortical Plate	3	502608925	489115991	362837579	hg19	GSM2054566	(Won et al. 2016)
Cortical Plate	**merged**	**1851585646**	**1814870338**	**1319302868**			
Germinal Zone	1	682518562	675056439	487874057	hg19	GSM2054567	(Won et al. 2016)
Germinal Zone	2	696799199	689981271	503166075	hg19	GSM2054568	(Won et al. 2016)
Germinal Zone	3	523694404	512704502	384384534	hg19	GSM2054569	(Won et al. 2016)
Germinal Zone	**merged**	**1903012165**	**1877742212**	**1375424666**			

Table S6 – 5C Loop Calls

Provided in separate spreadsheet.

Table S7 – Summary of new ChIP-seq datasets provided in this study

Target	Condition	Cell Type	Mapped Test ChIP-seq Reads	Number non-redundant tags utilized (after down-sampling)	Control Samples	Mapped Control ChIP-seq Reads	Number non-redundant tags utilized (after down-sampling)
H3K27ac	Bic	Cortical Neuron	41021267	38000000	Bic Treated Cortical Neuron	47530457	44000000
H3K27ac	TTX	Cortical Neuron	56699076	38000000	TTX Treated Cortical Neuron	52796934	44000000

H3K27ac	Untreat	Cortical Neuron	66252853	38000000	Untreated Cortical Neuron	83933042	44000000

Table S8 – H3K27ac Peaks called in the Bic condition (called using MACS2 --broad, pvalue and broadPeak cutoff thresholds = 1e-8)

Provided in separate spreadsheet.

Table S9 – H3K27ac Peaks called in the Untreat condition (called using MACS2 --broad, pvalue and broadPeak cutoff thresholds = 1e-8)

Provided in separate spreadsheet.

Table S10 – H3K27ac Peaks called in the TTX condition (called using MACS2 --broad, pvalue and broadPeak cutoff thresholds = 1e-8)

Provided in separate spreadsheet.

Table S11 – Putative distal enhancer regions parsed as being Bic-specific based on H3K27ac signal

Provided in separate spreadsheet.

Table S12 – Putative distal enhancer regions parsed as being activity invariant based on H3K27ac signal

Provided in separate spreadsheet.

Table S13 – Putative distal enhancer regions parsed as being TTX-specific based on H3K27ac signal

Provided in separate spreadsheet.

Table S14 – Loops called on mouse ES cell HiC from Bonev et al. 2017

Provided in separate spreadsheet.

Table S15 – Loops called on mouse NPC HiC from Bonev et al. 2017

Provided in separate spreadsheet.

Table S16 – Loops called on mouse cortical neuron (CN) HiC from Bonev et al. 2017

Provided in separate spreadsheet.

Table S17 - Loops called on human cortical plate (CP) tissue HiC from Won et al. 2016

Provided in separate spreadsheet.

Table S18 - Loops called on human germinal zone (GZ) tissue HiC from Won et al. 2016

Provided in separate spreadsheet.

Table S19 - Classified genes opposite disease-Associated SNVs

Provided in separate spreadsheet.